IEEE Access
Multidisciplinary | Rapid Review | Open Access Journal

Received February 17, 2019, accepted March 4, 2019, date of current version May 1, 2019.

Digital Object Identifier 10.1109/ACCESS.2019.2903726

Effect of Wiring and Cabling Topologies on the Performance of Distributed MIMO OFDM VLC Systems

OMER NARMANLIOGLU[1], (Student Member, IEEE), REFIK CAGLAR KIZILIRMAK[2], (Member, IEEE), FARSHAD MIRAMIRKHANI[1], (Student Member, IEEE), SADI SAFARALIEV[1,3], (Student Member, IEEE), SADIQ M. SAIT[4], (Senior Member, IEEE), AND MURAT UYSAL[1], (Fellow, IEEE)

[1]Department of Electrical and Electronics Engineering, Ozyegin University, 34794 Istanbul, Turkey
[2]Department of Electrical and Computer Engineering, Nazarbayev University, 010000 Astana, Kazakhstan
[3]Vestel Electronics Company, 45030 Manisa, Turkey
[4]Center for Communications and IT Research, Research Institute, King Fahd University of Petroleum & Minerals, Dhahran 31261, Saudi Arabia

Corresponding author: Omer Narmanlioglu (omer.narmanlioglu@ozu.edu.tr)

The work of R. C. Kizilirmak was supported by the Nazarbayev University through a research grant. The work of S. M. Sait was supported by the King Fahd University of Petroleum and Minerals, Dhahran, Saudi Arabia. The work of M. Uysal was supported by the Turkish Scientific and Research Council (TUBITAK) under Grant 215E311.

ABSTRACT Since most indoor spaces have multiple luminaires for illumination, for visible light communication (VLC) systems, multiple-input multiple-output (MIMO) communication emerges as a natural solution to improve the data rates and/or the link reliability. The existing works on MIMO VLC systems, however, overlook the characteristics of the lighting infrastructure and the luminaire design, which might have implications for the VLC system design. A luminaire typically consists of multiple LED chips. The wiring topology refers to how the LED chips are connected within the luminaire. The cabling topology, on the other hand, refers to how the luminaires are connected to the communication access point (AP). Based on the type and length of cabling and wiring, significant delays can be introduced, which should be taken into account in channel modeling. In this paper, we adopt the non-sequential ray tracing to model the distributed MIMO VLC channels for various practical wiring and cabling topologies. Based on the developed channel models, we provide a comparative performance analysis of repetition coding (RC), spatial multiplexing (SMUX), and spatial modulation (SMOD) MIMO modes. Our results quantify the effect of wiring/cabling delays and provide insights into the optimized design of lighting infrastructure and luminaires for the support of VLC as an add-on service.

INDEX TERMS Visible light communication, multiple-input multiple-output, OFDM, channel modeling, cabling delay.

I. INTRODUCTION

Visible light communication (VLC) is an indoor wireless access technology considered as an alternative or complementary to radio-frequency (RF) counterparts [1]. VLC relies on intensity modulation and direct detection (IM/DD) where the information is transmitted via light intensity by light emitting diodes (LEDs) at the transmitter and recovered by photodetectors (PDs) at the receiver. In IM/DD, the information signal must be real-valued and non-negative. In order to satisfy these constraints, earlier works on VLC considered pulse modulation techniques. Later, multi-carrier VLC communication was proposed to boost the data rate on VLC channels with frequency-selective characteristics. Different optical orthogonal frequency division multiplexing (OFDM) methods such as direct current biased

The associate editor coordinating the review of this manuscript and approving it for publication was Franco Fuschini.

optical OFDM (DCO-OFDM) [2], asymmetrically-clipped optical OFDM (ACO-OFDM) [3], flip-OFDM [4], unipolar OFDM (U-OFDM) [5]) and its enhanced version, and, enhanced U-OFDM (eU-OFDM) [6] have been proposed to satisfy the constraints of IM/DD transmission.

Multiple-input multiple-output (MIMO) transmission techniques can be employed to further improve data rates and/or link reliability. For indoor VLC systems, MIMO emerges as a natural solution since most indoor spaces already have multiple luminaires for illumination. Several VLC studies [7]–[15] have already investigated MIMO techniques for VLC. In [7], three MIMO techniques namely, repetition coding (RC), spatial multiplexing (SMUX) and spatial modulation (SMOD) were investigated under the assumption of frequency-flat channels. A similar comparative analysis for OFDM-based MIMO systems was reported in [8]. In [9], the performance of MIMO-OFDM VLC system was analyzed in a multi-user setting. In [10], a new constellation design was proposed for a MIMO VLC system in an effect to improve error performance with respect to RC, SMUX and SMOD. In [11], the performance of SMUX was investigated using sub-optimal receivers and the effect of channel correlation was quantified. In [12], joint optimization of pre-coder and equalizer was proposed to combat influence of channel estimation imperfections in a MIMO VLC system with SMUX. Adaptive MIMO VLC systems were further proposed in [13]–[15], and here transmission parameters were selected based on the channel state information available at transmitter side.

Existing works on MIMO VLC systems consider the use of multiple luminaires as transmitters, effectively realizing a distributed MIMO implementation. These works implicitly assume ideal connections between luminaires as well as ideal connectivity within the chips of a luminaire. They mainly overlook the characteristics of lighting infrastructure and luminaire design that might have implications for VLC system design. A luminaire typically consists of multiple LED chips. Wiring topology refers to how LED chips are connected within the luminaire. Cabling topology, on the other hand, refers to how the luminaires are connected to the communication access point (AP). Based on the type and length of cabling/wiring, significant delays can get added, and these should be taken into account during channel modeling. To address such practical concerns, in this paper we analyze the impact of different wiring and cabling topologies on the performance of MIMO-OFDM based VLC systems. To the best of our knowledge, there is only one previous work that discusses the effect of cabling and wiring topologies [16]. The work in [16] is however limited to the assumptions of only purely diffuse reflections and ideal Lambertian source which might not hold true in many practical cases. In this work, we adopt non-sequential ray tracing to model distributed MIMO VLC channels taking into account wiring and cabling delays. Based on the developed channel models, we evaluate and compare the bit error rate (BER) performances of RC, SMUX and SMOD MIMO modes for DCO-OFDM.

The rest of this paper is organized as follows. In Section II, we describe the channel modeling approach and introduce the indoor MIMO VLC channel models discussing the impact of wiring and cabling topology on the channel characteristics. In Section III, we present the MIMO-OFDM based VLC system under consideration and analyze the performance of RC, SMUX and SMOD. In Section IV, we present the numerical results for error rate performance. Finally, we conclude the paper in Section V.

Notation: $||.||^2$, $(.)^*$ and $[.]^{\mathrm{T}}$ denote Euclidean distance, complex conjugate and transpose respectively. $\otimes$ is convolution operator, $\delta(t)$ is the Dirac delta function, and $Q(.)$ is the tail probability of standard normal distribution.

II. MIMO VLC CHANNEL MODELS

A. CHANNEL MODELING APPROACH

For channel modeling, we take advantage of the ray tracing features of optical design software Zemax® [17]. The simulation environment is created in Zemax® and enables one to specify the geometry of the environment, the objects within, as well as the specifications of the sources (i.e., LEDs) and receivers (i.e., PDs). For a given number of rays and the number of reflections, the non-sequential ray tracing tool calculates the detected power and path lengths from source to detector for each ray. These are then imported to Matlab® and processed to yield the channel impulse response (CIR).

In this work, we assume that there are multiple ceiling luminaires in the environment where each LED luminaire consists of multi LED chips. Assume that there are N_L luminaires and each luminaire includes N_C LED chips. Let $h_i(t)$, $i = 1, \ldots, N_C$ denote the individual optical CIR between the i^{th} LED chip and the receiver. It can be expressed as

$$h_i(t) = \sum_{j=1}^{N_r} P_{i,j}\, \delta(t - \tau_{i,j}) \tag{1}$$

where $P_{i,j}$ is the optical power of the j^{th} ray from the i^{th} LED chip, $\tau_{i,j}$ is the propagation time of the j^{th} ray from the i^{th} LED chip, and N_r is the number of rays received at the detector. The optical CIR between the k^{th} luminaire $k = 1, \ldots, N_L$ and the receiver can be expressed as

$$h_k(t) = \sum_{i=1}^{N_C} h_i(t - \tau_{W_i}) \tag{2}$$

where τ_{W_i} is the wiring delay of the i^{th} LED chip and N_C is the number of LED chips inside the k^{th} luminaire.

The overall optical CIR is then given as

$$\begin{aligned} h(t) &= \sum_{k=1}^{N_L} h_k(t - \tau_{C_k}) \\ &= \sum_{k=1}^{N_L} \sum_{i=1}^{N_C} \sum_{j=1}^{N_r} P_{i,j}\, \delta(t - \tau_{i,j} - \tau_{W_i} - \tau_{C_k}) \end{aligned} \tag{3}$$

where τ_{C_k} is the cabling delay of the k^{th} luminaire and N_L is the number of ceiling luminaires. The frequency response of the optical channel can be further obtained through the Fourier transform, i.e.,

$$H(f) = F[h(t)] = \int_{-\infty}^{\infty} \sum_{k=1}^{N_L} \sum_{i=1}^{N_C} \sum_{j=1}^{N_r} P_{i,j}\, \delta(t - \tau_{i,j} - \tau_{W_i} - \tau_{C_k}) e^{-j2\pi t} dt. \tag{4}$$

B. CABLING AND WIRING TOPOLOGY

We consider two cabling topologies where the data/electrical cables are terminated at the middle of luminaires. In the first topology (Fig. 1a), the length of cable between the access point and each luminaire is the same. In the second topology (Fig. 1b), the length of cable for each luminaire changes. Difference in two topologies will not have any effect on illumination performance but the communication performance might be affected due to different cable lengths. For instance, when a signal is sent from AP to luminaires, all of the luminaires in Fig. 1a would receive it at the same time. On the other hand, in Fig. 1b, luminaire pairs (L_2 and L_3) and (L_1 and L_4) would receive it at the same time while there would be a particular delay between two pairs based on the cable length differences.

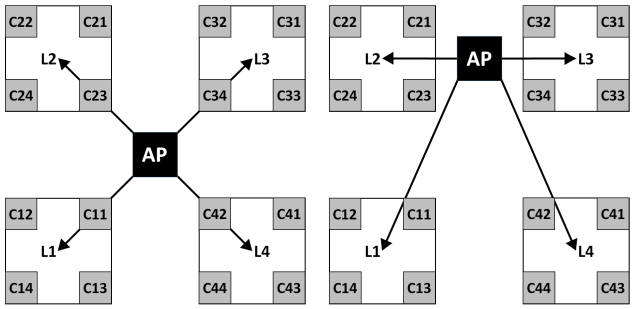

FIGURE 1. Cabling topologies under consideration (a) cabling topology I and (b) cabling topology II.

The wiring topology is more complicated than the cabling topology. In a LED luminaire, the LED chips can be connected in series, in parallel, or in some combinations of series and parallel. The choice of wiring topology mainly depends on the number and characteristics of LED chips, their driving forward current (I_f), and forward voltage (V_f), as well as the output current and voltage of the power supply unit (PSU) in the LED luminaire. There are two types of PSUs, i.e., constant current PSUs and constant voltage PSUs. A constant current PSU has an output of fixed current with a variable voltage within a particular range. These PSUs vary the voltage with respect to load while keeping the current constant. On the other hand, a constant voltage PSU does the reverse, i.e., varies the current within a range while keeping the output voltage constant. In LEDs, because of the significant changes in I_f and relative luminous flux with small changes in V_f, constant current PSUs are typically preferred to have more control over total light output of luminaires and uniformity of light output. Therefore, all of the LED chips are typically driven at the same forward current.

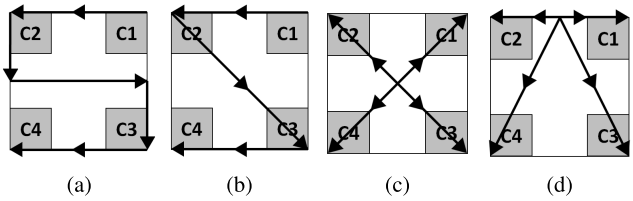

FIGURE 2. Wiring topologies under consideration (a) wiring topology I, (b) wiring topology II, (c) wiring topology III and (d) wiring topology IV.

According to the above considerations, four typical wiring topologies are presented in Fig. 2. In Figs. 2a and 2b, four LED chips C_i, $i = 1, \ldots, 4$ are connected in series. In Figs. 2c and 2d, LED chips are connected in parallel. In Figs. 2a and 2b, all of the four LED chips would have the same I_f as desired for uniform illumination. In Figs. 2c and 2d, all of the four LED chips would have the same V_f values. This indicates that similar I_f values will flow through each LED chip if their V_f differences are sufficiently low.

C. CHANNEL IMPULSE RESPONSES

We consider a MIMO system with $N_L = 4$ luminaires and $N_R = 4$ PDs employed in a room with dimensions of 5 m $\times$ 5 m $\times$ 3 m as shown in Fig. 3a with plaster ceiling/walls and pinewood floor. Four luminaires denoted as L_k, $k = 1, \ldots, 4$ are placed on the ceiling with equidistant spacing of 2 m. Each luminaire has a square shape with size of 0.6 m $\times$ 0.6 m and consists of 4 LED chips denoted as $C_{k,i}$, $i = 1, \ldots, 4$. Each LED chip radiates 5 W with a view angle of 120°. The receiver is designed in the form of a flat-top pyramid (see Fig.3.b) with four PDs to provide a wide angle reception, and to take advantage of the angular and spatial diversity [14], [18], [19]. The receiver is placed on the table at a height of 0.8 m. The field-of-views (FOVs) semi-angle and area of the PD are 85° and 1 cm^2, respectively. The propagation delay for the wires within the luminaire is assumed to be $\tau_{W_i} = 6.5$ ns/m [20]. We assume the deployment of CAT5 as the data cable and consider a propagation delay of $\tau_{C_k} = 5$ ns/m [21].

First, we only consider the effect of cabling topologies and neglect the wiring delays.[1] As a benchmark, we further consider the hypothetical case where the cables are delay-free. The overall optical CIR $h(t)$ as seen by the photodetector D_1 is presented in Fig. 4 for two different cabling topologies under consideration. In topology I (Fig. 4a), we have one large peak and then one small. Since the cabling delays of four luminaires are the same, the signals from each luminaire

[1] It should be noted that the attenuation in data cables is neglected. In practice, an amplifier is employed at VLC-enabled LED luminaire to mitigate the effect of such losses.

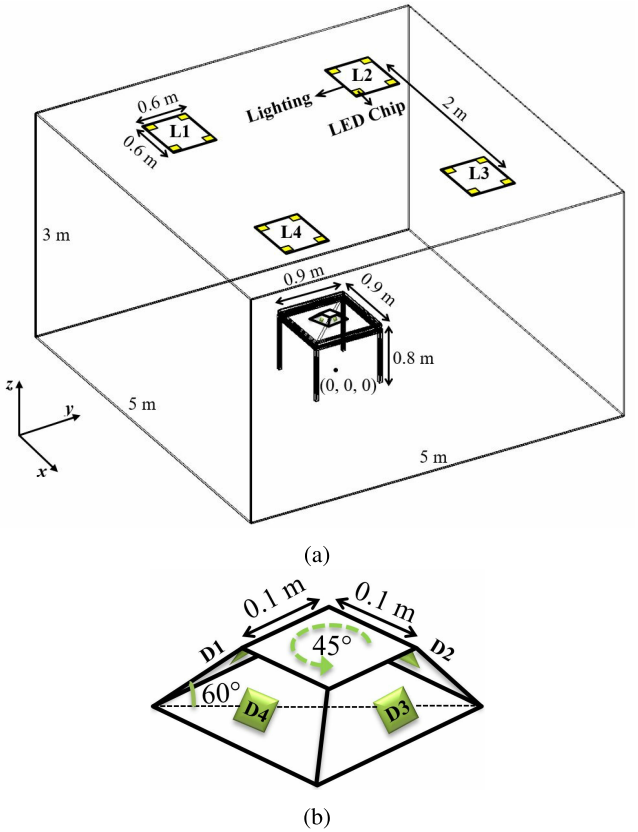

FIGURE 3. (a) MIMO VLC system under consideration and (b) zoomed version of receiver.

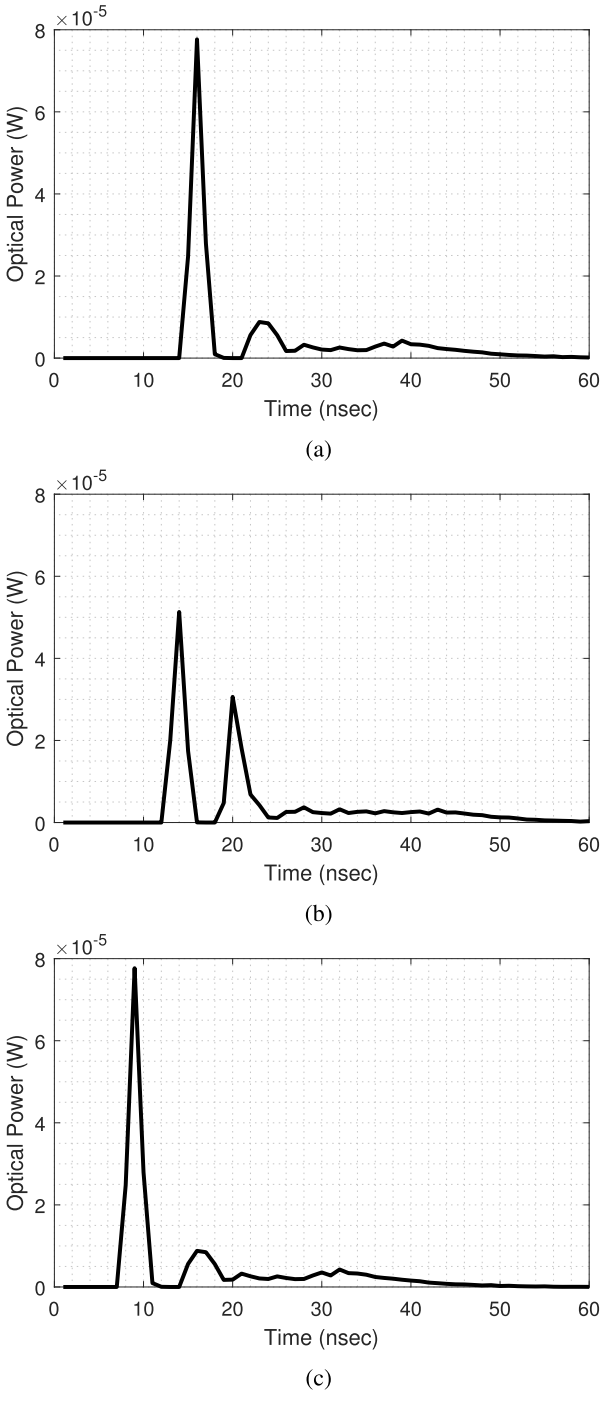

FIGURE 4. Overall optical CIRs (as received by the photodetector D_1) for (a) cabling topology I, (b) cabling topology II and (c) delay-free cabling.

are received at the same time. This results in one large peak followed by a small peak where the latter results from multipath reflections. In topology II (Fig. 4b), it is observed that we have two large peaks followed by a small one. The first large peak is the joint contribution of luminaires L_2 and L_3 since the associated delays are the same and the signals emitted from these luminaires are received at the same time. Similarly, the second large peak is the joint contribution of luminaires L_1 and L_4. For the hypothetical case where the cables are delay-free (Fig. 4c), we have one large peak followed by a small one similar to topology I. However, the large peak in this case occurs at 9 ns while the large peak in topology I occurs at 16 ns which is the result of cabling delay.

Second, we only consider the effect of wiring topologies and neglect the cabling delays. As a benchmark, we further consider the hypothetical case where the wires are delay-free. The optical CIR $h_1(t)$ between luminaire L_1 and photodetector D_1 is presented in Fig. 5. It is observed from Figs. 5a and 5b that in wiring topologies I and II, we have four large peaks followed by a small one. Four large peaks come from LED chips $C_{1,1}$, $C_{1,2}$, $C_{1,3}$ and $C_{1,4}$ while the small one results from multipath reflections. In topology III (see Fig. 5c), it is observed that we have one large peak and then one small. This is as a result of the fact that the wiring delays of four LED chips are the same. In topology IV (see Fig. 5d), it is observed that we have two large peaks and then one small. Two large peaks come from LED chip pairs ($C_{1,1}$ and $C_{1,2}$) and ($C_{1,3}$ and $C_{1,4}$). For the hypothetical delay-free case, we have one large peak and then one small similar to topology III. It should be noted that the large peak in this case occurs at 9 ns, however, the large peak in topology III occurs at 13 ns which is the result of wiring delay.

Finally, we consider the joint effect of both wiring and cabling topologies in Fig. 6. We assume the use of cabling

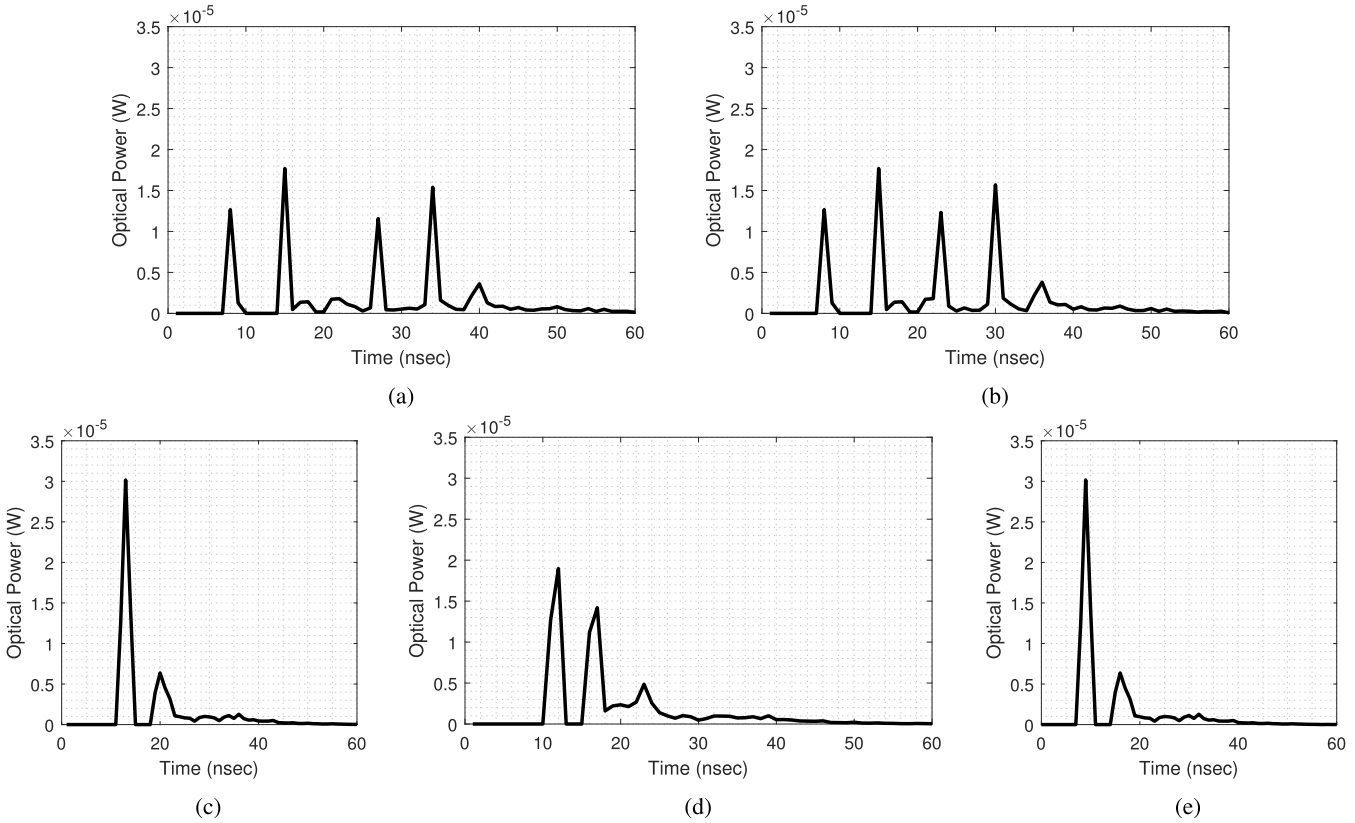

FIGURE 5. Optical CIRs from the luminaire L_1 (as received by the photodetector D_1) for (a) wiring topology I, (b) wiring topology II, (c) wiring topology III, (d) wiring topology IV and (e) delay-free wiring.

topology I in conjunction with wiring topology I and III. It is observed from Fig. 6a. that for cabling topology I in conjunction with wiring topology I, we have four large peaks followed by a small one. The CIR is similar to what is obtained for wiring topology presented in Fig. 5a. This indicates that the wiring topology is dominant for the channel characterization. Since the CIR shown in Fig. 6a is composed of the CIRs from four luminaires, its amplitude is larger than that one shown in Fig. 5a. Additionally, the first peak in the CIR presented in Fig. 5a (where wiring topology I is considered and cabling delay is ignored) occurs at 8 ns while the first peak of CIR in Fig. 6a (where the combined effect of cabling topology I and wiring topology I is considered) occurs at 15 ns as a result of cabling delay. It is further observed from the comparison of Fig. 6b and Fig. 6c that the CIR for the case of cabling topology I and wiring topology III have a similar behavior to the ideal case with only some delays. This is a result of the fact that cabling topology I and wiring topology III have symmetrical structures. In other word, all luminaires in cabling topology I and all LED chips in wiring topology III have identical cabling and wiring delays, respectively. Such a symmetrical wiring/cabling structure results in only an overall shift of the CIR.

The corresponding channel frequency and phase responses of overall CIRs for these three cases are further illustrated in Fig. 7. It is observed that frequency selectivity is introduced with respect to the ideal case of delay-free wiring and cabling. This will introduce limitations on the transmission bandwidth. According to the well known 3-dB bandwidth definition [22], the bandwidth for the ideal case can be calculated as 12.74 MHz. This remains the same for the case where cabling topology I and wiring topology III are considered due to symmetrical structure. This reduces to 9.70 MHz for cabling topology I and wiring topology I where frequency selectivity is more pronounced. The difference can be seen in Fig. 7b where the delay introduced by wiring changes the phase response.

III. SYSTEM MODEL AND PERFORMANCE ANALYSIS

A. SYSTEM MODEL

Our system model is based on DCO-OFDM [2] which was adopted as the mandatory physical layer in the IEEE 802.15.13 standard [23]. OFDM is a multi-carrier communication technique and converts the frequency-selective channel into a number of frequency-flat sub-channels, therefore single-tap equalizers can be used for each sub-channel. Eliminating the need for complex equalizers, OFDM provides advantages over single-carrier systems and becomes our system choice here.

In DCO-OFDM, the binary information is first mapped to complex symbols $[s_1\ s_2\ s_3\ \ldots\ s_{N/2-1}]$ using phase-shift keying (PSK) or quadrature amplitude modulation (QAM)

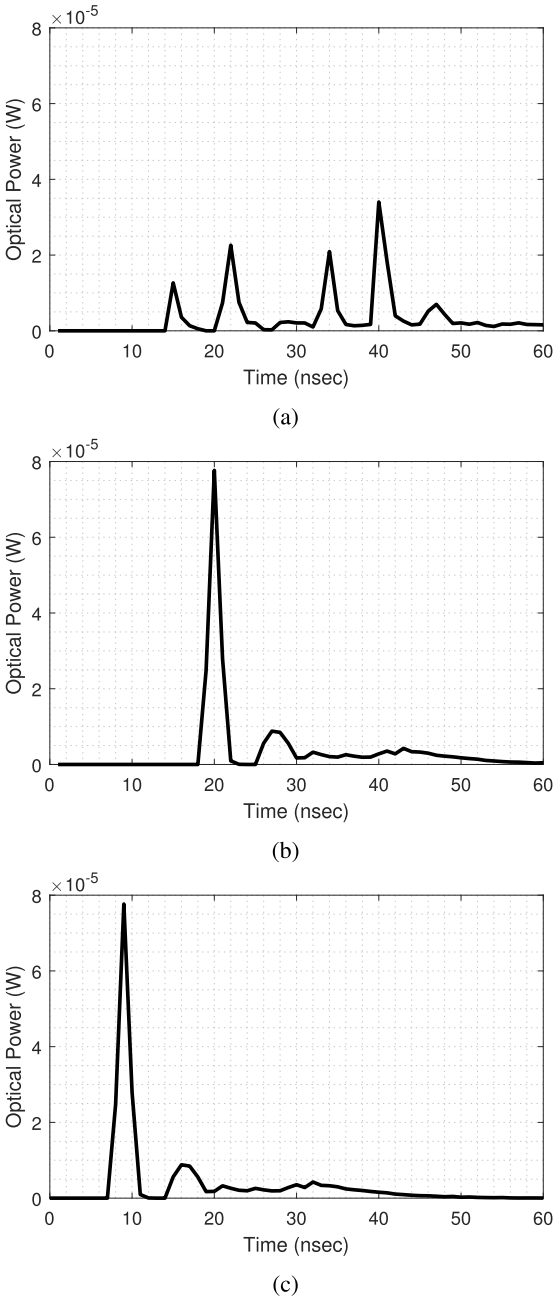

FIGURE 6. Overall optical CIRs (as received by the photodetector D_1) for (a) cabling topology I and wiring topology II and (b) cabling topology I and wiring topology III and (c) delay-free cabling and wiring.

where N is OFDM frame size. Then they are re-arranged satisfying Hermitian symmetry as

$$X = [0\ s_1\ s_2\ s_3\ \ldots\ s_{N/2-1}\ 0\ s^*_{N/2-1}\ \ldots s^*_2\ s^*_1]^{\mathrm{T}}. \quad (5)$$

This ensures that the output of inverse fast Fourier transform (IFFT) is real valued. After appending the cyclic prefix and parallel-to-serial conversion, a DC bias is added to shift the signal to the dynamic range of the LED.

We consider a MIMO system with N_L luminaires and N_R PDs as described in Section II. Let $c_{nm}(t)$ and $h_{nm}(t)$

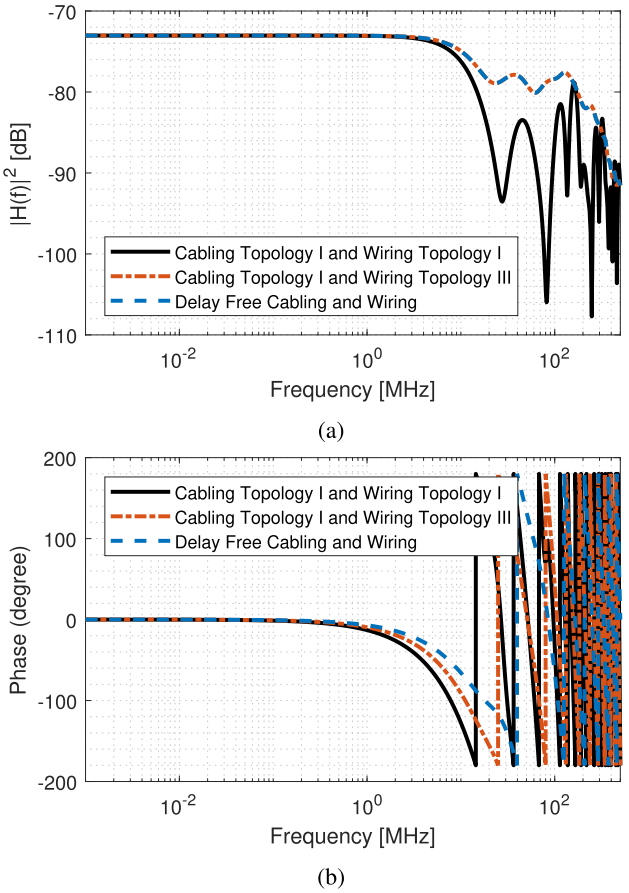

FIGURE 7. Channel frequency and phase responses of overall optical CIRs considering the combined effect of cabling and wiring delays.

respectively denote the optical and electrical CIRs from the m^{th} luminaire to the n^{th} PD. Under the assumption that electrical-to-optical conversion is ideal with unity gain, they are related to each other as,

$$h_{nm}(t) = g_{tx}(t) \otimes c_{nm}(t) \otimes g_{rx}(t),\ n \in \{1..N_R\}, m \in \{1..N_L\}, \quad (6)$$

where $g_{tx}(t)$ and $g_{rx}(t)$ are transmit and receive matched-filter responses, respectively. The received signal at the n^{th} PD can be written as

$$y_n(t) = \sum_{m=1}^{N_L} x_m(t) \otimes h_{nm}(t) + v_n(t),\ n \in \{1..N_R\}, \quad (7)$$

where $x_m(t)$ is the transmitted signal from the m^{th} luminaire and $v_n(t)$ is additive white Gaussian noise (AWGN) term with zero mean and N_0W variance at the n^{th} PD. The output of the FFT block

$$Y_n[k] = \sum_{m=1}^{N_L} X_m[k]H_{nm}[k] + V_n[k],\ n \in \{1..N_R\}, \quad (8)$$

where $V_n[k]$ is AWGN with the same statistics as $v_n(t)$. In (8), $H_{nm}[k]$ is the Fast Fourier Transform (FFT) response

of $h_{nm}(nT_S - \tau_{\text{offset}})$ where T_S is the sampling interval and

$$\tau_{\text{offset}} = \underset{i}{\text{argmax}} \left[\sum_{n=-\infty}^{\infty} |h_{nm}(t - nT_S - i)|^2 \right], \quad (9)$$

is the offset variable in order to maximize the energy of $h_{nm}[n]$ at the output [24].

We consider three different MIMO techniques, namely RC, SMUX and SMOD. In RC mode, each luminaire emits the same information to extract diversity gain. The Maximum Likelihood (ML) decision rule in this case can be written as

$$\hat{X}[k] = \underset{X[k]\in\Omega}{\text{argmin}} \left(\sum_{n=1}^{N_R} \left\| Y_n[k] - X[k] \sum_{m=1}^{N_L} H_{nm}[k] \right\|^2 \right), \quad (10)$$

where Ω is the set of constellation points. DCO-OFDM in RC mode achieves the spectral efficiency (SE) of $(\log_2 M)/2$ bit/sec/Hz (for large N), where M is modulation order.

In SMUX mode, each luminaire emits different information. Unlike RC, SMUX provides multiplexing gain but not diversity gain. Let $X[k] = [X_1[k]\ X_2[k]\ \ldots\ X_{N_L}[k]]^{\text{T}}$ denote the transmitted signal vector at the k^{th} subcarrier with a dimension of N_L. The ML decision rule can be written as

$$\hat{X}[k] = \underset{X\in\Phi}{\text{argmin}} \left(\|Y[k] - H[k]X\|^2 \right), \quad (11)$$

where $Y[k] = [Y_1[k]\ Y_2[k]\ \ldots\ Y_{N_R}[k]]^{\text{T}}$ is the received signal vector with the dimension of N_R, H $[k]$ is N_RxN_L channel matrix on the k^{th} subcarrier and Φ includes all possible combinations of transmitted signal vectors. The SE of DCO-OFDM in SMUX mode is $(\min(N_L, N_R)\log_2 M)/2$ bit/s/Hz (for large N).

In SMOD, luminaire index is used as an additional modulation dimension. Therefore, the binary information is mapped to complex symbols and LED array index [7]. At the input of the IFFT, after complex symbol mapping, conventional DCO-OFDM processes are performed. The ML decision rule is written as

$$\hat{X}[k] = \underset{X\in\Psi}{\text{argmin}} \left(\|Y[k] - H[k]X\|^2 \right), \quad (12)$$

where Ψ denotes the combination of constellation points and spatial dimension. Under ML detection, an exhaustive search of MN_L is done to find the closest outcome. DCO-OFDM with SMOD provides an SE of $(\log_2 N_L + \log_2 M)/2$ bit/s/Hz (for large N).

B. BER ANALYSIS

The overall BER for each MIMO mode can be calculated by taking the average of BER values, denoted by $\overline{\text{BER}}$, over the data subcarriers that are the first half of the frame except the DC subcarrier. Mathematically speaking, $\overline{\text{BER}}$ can be written as

$$\overline{\text{BER}} = \frac{2}{N-2} \sum_{k=1}^{N/2-1} \text{BER}[k] \quad (13)$$

where $\text{BER}[k]$ for RC mode is given by (15), as shown at the bottom of this page. Here, subcarrier-based signal-to-noise ratio (SNR) can be calculated by

$$\text{SNR}[k] = \frac{P \sum_{n=1}^{N_R} \left| \left(\sum_{m=1}^{N_L} H_{nm}[k] \right) \right|^2}{N_0 W N_L} \quad (14)$$

where P is average electrical power for transmission.

In SMUX mode, $\text{BER}[k]$ in (13) refers to upper bounded subcarrier-based BER given by (16), as shown at the bottom of this page, where $\text{d}_{\text{H}}(b_{m_1}, b_{m_2})$ is Hamming distance of two bit assignments, which are b_{m_1} and b_{m_2}, of the signal vectors s_{m_1} and s_{m_2}.

Finally for SMOD mode, $\text{BER}[k]$ in (13) refers to upper bounded subcarrier-based BER given by (17), as shown at the bottom of this page. In (17), $b_{m_1 n_{T1}}, b_{m_2 n_{T2}}$ are two different bit assignments with respect to constellation points (s_{m_1} and s_{m_2}) and transmitter indexes (n_{T1}, n_{T2}).

IV. NUMERICAL RESULTS

In this section, we present the BER performances of different MIMO modes under different cabling and wiring topologies. The evaluations are performed at a fixed SE of 4 bits/sec/Hz for a fair comparison among different

$$\text{BER}_{\text{RC}}[k] \approx \begin{cases} Q\left(\sqrt{2\text{SNR}[k]}\right) & , \text{B - PSK} \\ \frac{2\left(\sqrt{M}-1\right)}{\sqrt{M}\log_2\sqrt{M}} Q\left(\sqrt{\frac{3\text{SNR}[k]}{(M-1)}}\right) & , \text{square}-M-\text{QAM} \\ \frac{2}{\log_2(U\text{x}J)}\left[\frac{U-1}{U} Q\left(\sqrt{\frac{6\text{SNR}[k]}{U^2+J^2-2}}\right) + \frac{J-1}{J} Q\left(\sqrt{\frac{6\text{SNR}[k]}{U^2+J^2-2}}\right)\right] & , \text{rectangular}-M = U\text{x}J-\text{QAM} \end{cases} \quad (15)$$

$$\text{BER}_{\text{SMUX}}[k] \leq \frac{1}{M^{N_L}\log_2\left(M^{N_L}\right)} \sum_{m_1=1}^{M^{N_L}} \left(\sum_{m_2=1}^{M^{N_L}} d_{\text{H}}\left(b_{m_1}, b_{m_2}\right) Q\left(\sqrt{\frac{P}{2N_0 W N_L} \left\| H[k]\left(s_{m_1} - s_{m_1}\right) \right\|^2} \right) \right) \quad (16)$$

$$\text{BER}_{\text{SMOD}}[k] \leq \frac{1}{MN_L\log_2\left(MN_L\right)} \sum_{m_1=1}^{M} \left(\sum_{n_{T1}=1}^{N_L} \left(\sum_{m_2=1}^{M} \left(\sum_{n_{T2}=1}^{N_L} d_H\left(b_{m_1 n_{T1}}, b_{m_2 n_{T2}}\right) \right.\right.\right.$$
$$\left.\left.\left. \times\ Q\left(\sqrt{\frac{P}{2N_0 W} \sum_{n_R=1}^{N_R} \left| s_{m_2} H_{n_R n_{T2}}[k] - s_{m_1} H_{n_R n_{T1}}[k] \right|^2} \right) \right) \right) \right) \quad (17)$$

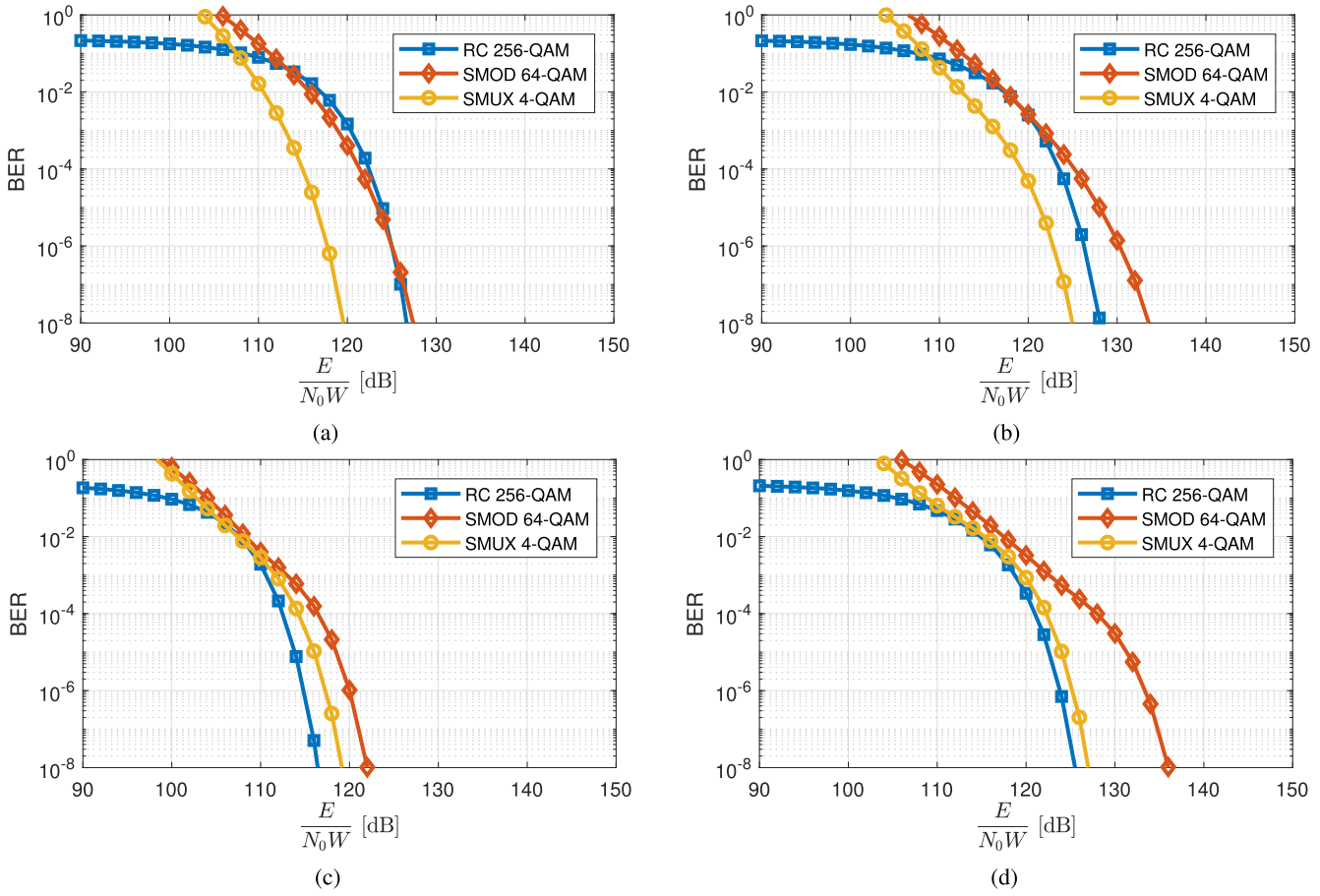

FIGURE 8. BER performance of RC, SMUX and SMOD for cabling topology I in conjunctuon with (a) wiring topology I, (b) wiring topology II, (c) wiring topology III, and (d) wiring topology IV.

MIMO modes. To achieve an SE of 4.0 bit/sec/Hz, 256-QAM, 16-QAM and 4-QAM are deployed respectively for RC, SMUX and SMOD modes. Square root raised cosine (SRRC) with unit roll-off factor is considered as transmit and receive matched filter. Sampling interval (T_S), noise density (N_0), number of subcarriers (N), cyclic prefix length are respectively set at 5 ns, 10^{-22} W/Hz, 256 and 24, and target BER is selected as 10^{-6}. The results are given in terms of transmit SNR which can be calculated based on E/N_0W.

Fig. 8 shows the BER performances of RC, SMUX and SMOD MIMO modes for different wiring topologies under the assumption of delay-free cabling between luminaires, e.g., cabling topology I. It is observed that SMUX outperforms RC and SMOD with the gains of approximately 7 dB for the wiring topology I (see Fig. 8a). It should be noted that the delay among the LED chips is the highest for wiring topology I over the other three topologies. For the wiring topology II (see Fig. 8b), where there is relatively less delay among the LED chips, the gains of SMUX over RC and SMOD become 3 dB and 7 dB, respectively. Moreover, when there is no delay among the LED chips as in wiring topology III (see Fig. 8c), RC outperforms both SMOD and SMUX with the gains of 5 dB and 2.5 dB. The highest relative gain of RC over SMOD is achieved in this case. The reason is that the zero delay among both luminaires and LED chips increases the channel correlation and that brings worse SMUX performance. When wiring topology IV (see Fig. 8d) is considered, the gain of RC mode over SMOD and SMUX counterparts become approximately 10 dB and 2 dB. In wiring topology IV, SMUX performance increases and SMOD performance decreases in comparison to RC. The increase in SMUX performance with respect to RC mode in wiring topology IV is due to the less channel correlation than wiring topology III, as a consequence of the delay between the two LED chips.

The results in Fig. 8 also reveal that increased delay between the LED chips yields weaker channel correlation that is the major requirement to increase the performance of SMOD and particularly SMUX. When the delay decreases among the LED chips (as in wiring topology III), the gain of RC over both SMOD and SMUX increases. Furthermore, decreasing the delay among the LED chips results in higher channel gain since the multiple transmissions from different chips constitute a more robust single-tap channel.

In Fig. 9, we further compare the individual BER performances of RC, SMUX and SMOD MIMO modes with respect to different wiring topologies. The highest gain from RC is obtained in wiring topology III (see Fig. 9a) due to the fact

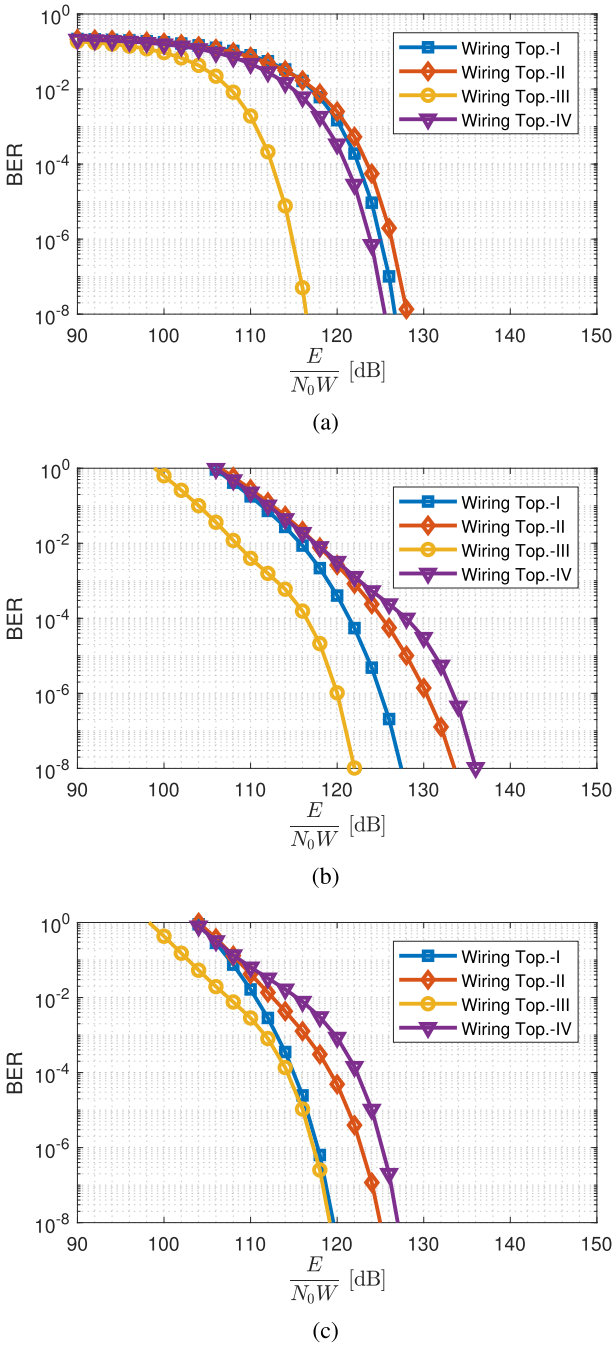

FIGURE 9. BER performance with different wiring topologies for (a) RC, (b) SMOD and (c) SMUX.

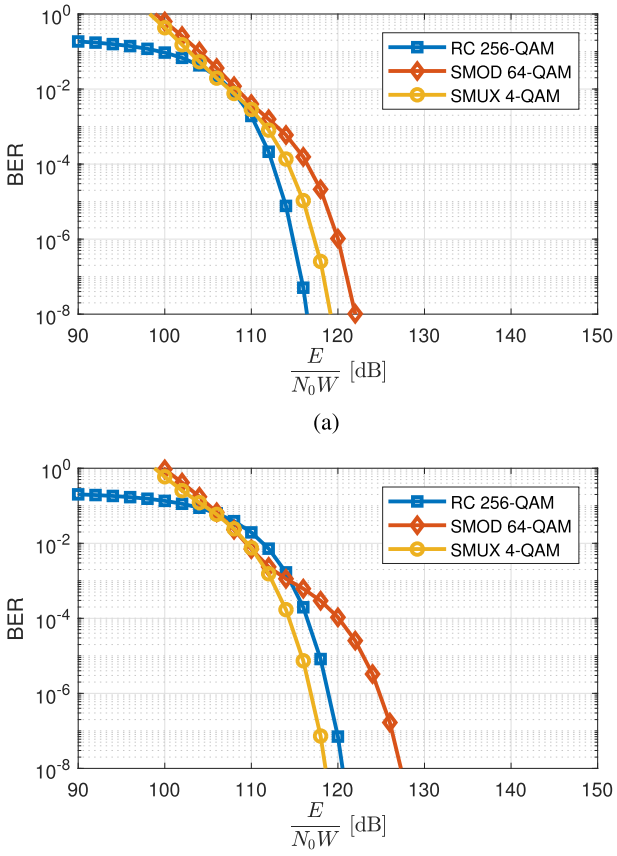

FIGURE 10. BER performance of RC, SMUX and SMOD under the consideration of cabling topology I with (a) cabling topology I and (b) cabling topology II.

that the zero delay among both luminaires and LED chips increases the channel gain. It is followed by topologies IV, I, and II with the gain penalty of 9 dB, 10 dB, and 11 dB. Same comparison is done for SMOD and SMUX modes in Figs 9b and 9c. Similar to RC, the highest performance is obtained in the wiring topology III where there is no delay between LEDs. For SMOD (see Fig. 9b) it is followed by topologies I, II, and IV with the gain penalty of 5 dB, 10 dB, and 13 dB, respectively. When we consider SMUX mode, gain difference between topology I and III is relatively small and they are followed by topology II and topology IV with the gain penalty of 5 dB, 7 dB.

In in Fig. 10, we evaluate the impact of different cabling topologies. We consider wiring topology III where there is no delay among the LED chips. It is observed that less delay among the luminaires (even zero for the cabling topology I) increases the channel correlation which leads better RC performance over both SMOD and SMUX (see Fig. 10a). In other words, RC outperforms SMOD with a gain of 5 dB and SMUX with 2.5 dB for cabling topology I. When cabling topology II (in which the L_1 and L_4, and L_2 and L_3 are synchronized) is considered (see Fig. 10b), the gain of RC over SMUX is decreased by 7 dB with respect to cabling topology I and SMUX outperforms RC mode with the gain of 2 dB. On the other hand, RC still outperforms SMOD with the approximately same amount of gain.

In Fig. 11, we compare the BER performances of RC, SMUX and SMOD MIMO modes with respect to different cabling topologies. The highest gain from RC and SMOD are obtained in cabling topology I (see Figs. 11a and 11b) since zero delay effectively increases the channel gain. On the other hand, for SMUX, the highest gain is obtained in cabling topology II with a relatively small gain difference, due to less channel correlation than cabling topology I, as a consequence of the delay between the luminaires.

As a final note, we emphasize that the above observations are reported for a room with a size of 5 m × 5 m × 3 m under

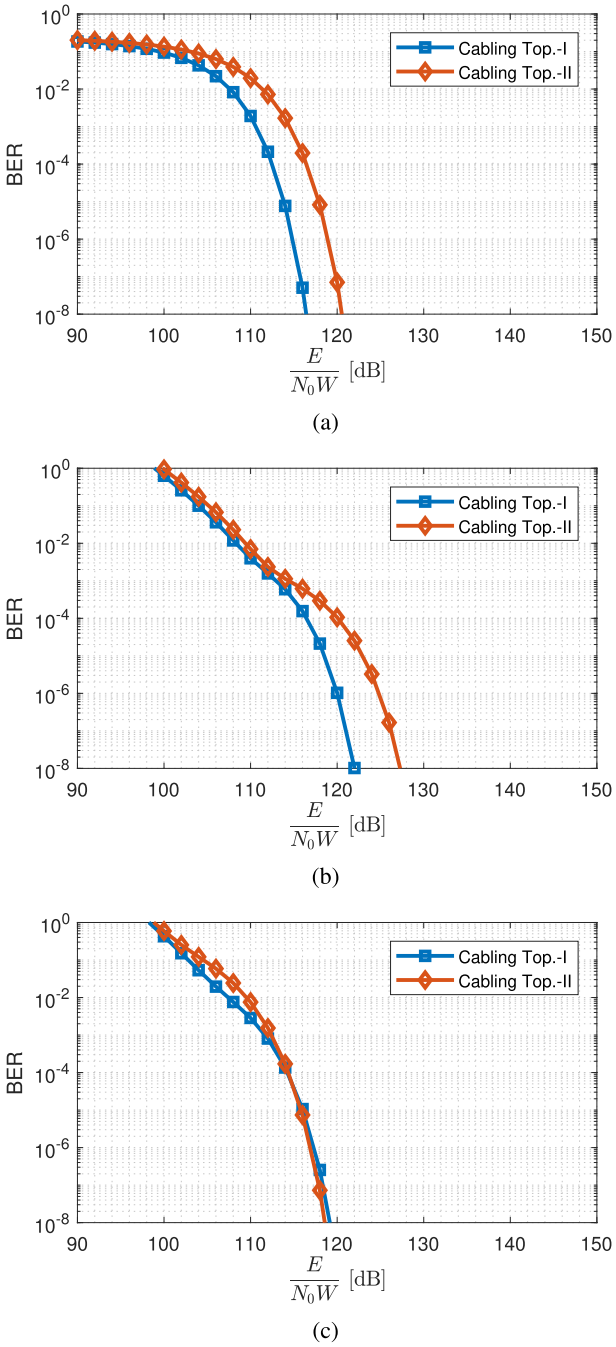

FIGURE 11. BER performance with different cabling topologies for (a) RC, (b) SMOD and (c) SMUX.

consideration. Different room sizes and shapes will change the cabling delay among luminaires. For example, if room size gets larger, lengths of cables will increase; therefore, more delays might be observed in CIRs. As long as the OFDM system parameters are selected properly taking into the delay spread of the channel, these can be effectively mitigated.

V. CONCLUSIONS

In this work, we have considered a MIMO OFDM VLC system and quantified the impact of cabling and wiring topologies on the system performance. In the first part of our paper, we have adopted non-sequential ray tracing and obtained CIRs for distributed MIMO VLC channels taking into account wiring and cabling delays. Our results point out that wiring topology is dominant on channel characteristics. Furthermore, it is found out that symmetrical wiring/cabling structures are more favorable to handle frequency-selectivity. It should be however emphasized that wiring and cabling choices are not necessarily in the hands of a VLC system designer. The LED manufacturer decides on the type of wiring within the luminaires. The cabling is either done by telecom operator or perhaps during building construction. Therefore, symmetric cabling/wiring cannot be always guaranteed.

In the second part of the paper, in an effort to highlight the degradation due to different wiring/cabling topologies, we presented comparative performance evaluation of RC, SMUX and SMOD MIMO modes based on the developed channel models. Our BER results reveal that RC suffers from the cabling delay as compared to other two MIMO modes. The cabling delay also degrades the performances of SMOD mode, however, it provides additional gain to the performance of SMUX. Moreover, SMOD and SMUX are less sensitive to cabling delays as compared to RC. Increase in the delay between the luminaires leads better performance results for SMOD and SMUX modes, due to less channel correlation on the receiver side. Based on the targeted application's quality of service (QoS) requirements, one may prefer to either improve link reliability (through increase in diversity gain) or throughput (through increase in multiplexing gain). Our results will help the system designer choose the proper MIMO scheme. Alternatively, one can design an adaptive system which switches between MIMO modes based on the channel state information and QoS requirements.

ACKNOWLEDGMENT

This paper was presented in part at the 10th International Conference on Electrical and Electronics Engineering (ELECO 2017).

REFERENCES

[1] S. Wu, H. Wang, and C. H. Youn, "Visible light communications for 5G wireless networking systems: From fixed to mobile communications," *IEEE Netw.*, vol. 28, no. 6, pp. 41–45, Nov. 2014.
[2] J. Armstrong, "OFDM for optical communications," *J. Lightw. Technol.*, vol. 27, no. 3, pp. 189–204, Feb. 1, 2009.
[3] J. Armstrong and A. J. Lowery, "Power efficient optical OFDM," *Electron. Lett.*, vol. 42, no. 6, pp. 370–372, Mar. 2006.
[4] N. Fernando, Y. Hong, and E. Viterbo, "Flip-OFDM for unipolar communication systems," *IEEE Trans. Commun.*, vol. 60, no. 12, pp. 3726–3733, Dec. 2012.
[5] D. Tsonev, S. Sinanovic, and H. Haas, "Novel unipolar orthogonal frequency division multiplexing (U-OFDM) for optical wireless," in *Proc. IEEE 75th Veh. Technol. Conf. (VTC Spring)*, May 2012, pp. 1–5.
[6] D. Tsonev, S. Videv, and H. Haas, "Unlocking spectral efficiency in intensity modulation and direct detection systems," *IEEE J. Sel. Areas Commun.*, vol. 33, no. 9, pp. 1758–1770, Sep. 2015.
[7] T. Fath and H. Haas, "Performance comparison of MIMO techniques for optical wireless communications in indoor environments," *IEEE Trans. Commun.*, vol. 61, no. 2, pp. 733–742, Feb. 2013.
[8] M. O. Damen, O. Narmanlioglu, and M. Uysal, "Comparative performance evaluation of MIMO visible light communication systems," in *Proc. 24th Signal Process. Commun. Appl. Conf. (SIU)*, May 2016, pp. 525–528.

[9] Q. Wang, Z. Wang, and L. Dai, "Multiuser MIMO-OFDM for visible light communications," *IEEE Photon. J.*, vol. 7, no. 6, pp. 1–11, Dec. 2015.

[10] Y.-J. Zhu, W.-F. Liang, J.-K. Zhang, and Y.-Y. Zhang, "Space-collaborative constellation designs for MIMO indoor visible light communications," *IEEE Photon. Technol. Lett.*, vol. 27, no. 15, pp. 1667–1670, Aug. 1, 2015.

[11] C. He, T. Q. Wang, and J. Armstrong, "Performance of optical receivers using photodetectors with different fields of view in a MIMO ACO-OFDM system," *J. Lightw. Technol.*, vol. 33, no. 23, pp. 4957–4967, Dec. 1, 2015.

[12] K. Ying, H. Qian, R. J. Baxley, and S. Yao, "Joint optimization of precoder and equalizer in MIMO VLC systems," *IEEE J. Sel. Areas Commun.*, vol. 33, no. 9, pp. 1949–1958, Sep. 2015.

[13] K.-H. Park, Y.-C. Ko, and M.-S. Alouini, "On the power and offset allocation for rate adaptation of spatial multiplexing in optical wireless MIMO channels," *IEEE Trans. Commun.*, vol. 61, no. 4, pp. 1535–1543, Apr. 2013.

[14] P. F. Mmbaga, J. Thompson, and H. Haas, "Performance analysis of indoor diffuse VLC MIMO channels using angular diversity detectors," *J. Lightw. Technol.*, vol. 34, no. 4, no. 4, pp. 1254–1266, Feb. 15, 2016.

[15] O. Narmanlioglu, R. C. Kizilirmak, T. Baykas, and M. Uysal, "Link adaptation for MIMO OFDM visible light communication systems," *IEEE Access*, vol. 5, pp. 26006–26014, 2017.

[16] G. Ren, S. He, and Y. Yang, "An improved recursive channel model for indoor visible light communication systems," *Inf. Technol. J.*, vol. 12, no. 6, pp. 1245–1250, 2013.

[17] F. Miramirkhani and M. Uysal, "Channel modeling and characterization for visible light communications," *IEEE Photon. J.*, vol. 7, no. 6, Dec. 2015.

[18] A. Burton, Z. Ghassemlooy, S. Rajbhandari, and S.-K. Liaw, "Design and analysis of an angular-segmented full-mobility visible light communications receiver," *Trans. Emerg. Telecommun. Technol.*, vol. 25, no. 6, pp. 591–599, 2014.

[19] A. Nuwanpriya, S.-W. Ho, and C. S. Chen, "Indoor MIMO visible light communications: Novel angle diversity receivers for mobile users," *IEEE J. Sel. Areas Commun.*, vol. 33, no. 9, pp. 1780–1792, Sep. 2015.

[20] H. Zumbahlen, "Printed circuit board (PCB) design issues," in *Basic Linear Design*. Norwood, MA, USA: Analog Devices, 2007, ch. 12.

[21] A. B. Semenov, S. K. Strizhakov, and I. R. Suncheley, "SCS electrical components," in *Structured Cable Systems*. New York, NY, USA: Springer, 2002, ch. 3.

[22] A. F. Molisch, *Wireless Communication*. Hoboken, NJ, USA: Wiley, 2012.

[23] N. Serafimovski and V. Jungnikel. *May IEEE 802.15.13 Minutes*. Accessed: Jun. 10, 2017. [Online]. Available: https://mentor.ieee.org/802.15/dcn/17/15-17-0311-00-0013-meeting-minutes-of-tg13-may-2017.docx,doc:IEEEP802.15-17-0311-00-0013

[24] C. R. Johnson, Jr., and W. A. Sethares, *Telecommunications Breakdown: Concepts of Communication Transmitted via Software-Defined Radio*. Upper Saddle River, NJ, USA: Prentice-Hall, 2004.

OMER NARMANLIOGLU received the B.Sc. degree from the Department of Electrical and Electronics Engineering, Bilkent University, Ankara, Turkey, in 2014, and the M.Sc. degree from Ozyegin University, Istanbul, Turkey, in 2016, where he is currently pursuing the Ph.D. degree. He is currently an RF & SON Consultant with P.I. Works. His research interests include the physical and link layer aspects of communication systems, self-organizing networks, and software-defined networking paradigm for radio access, transmission, and packet core networks. His major distinctions include Best Research Assistant Award from Ozyegin University, in 2016, the National Instruments Engineering Impact Award in Austin, Texas, USA, in 2017, and the Best Paper Award at the IEEE International Conference on the Network of the Future, London, U.K., in 2017.

REFIK CAGLAR KIZILIRMAK received the B.Sc. and M.Sc. degrees in electrical and electronics engineering from Bilkent University, Ankara, Turkey, in 2004 and 2006, respectively, and the Ph.D. degree from Keio University, Yokohama, Japan, in 2010. He worked on several telecommunication and defense industry projects with the Communications and Spectrum Management Research Center, Turkey. He is currently with the Department of Electrical and Electronics Engineering, Nazarbayev University, Astana, Kazakhstan. He contributed to the technical requirements document of 802.15.7r1 standardization, which will enable visible light communication. He holds three patent applications in the field of wireless communications to U.S. and Japan patent offices. He was a recipient of the IEEE VTS Japan 2008 Young Researcher's Award and the IEICE WBS Best Paper Award.

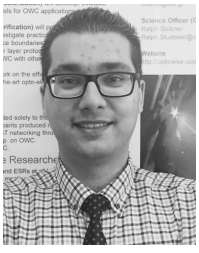

FARSHAD MIRAMIRKHANI received the B.Sc. degree (Hons.) in electrical and electronics and the M.Sc. degree (Hons.) in communication engineering from the University of Isfahan, Isfahan, Iran, in 2011 and 2014, respectively, and the Ph.D. degree in electrical and electronics engineering from Ozyegin University, Istanbul, Turkey, in 2018. He has also contributed to the standardization works of the IEEE 802.15.13 (Short-Range Optical Wireless Communications) and the IEEE 802.11bb (Light Communications for Wireless Local Area Networking). The Li-Fi channels developed by him and Prof. M. Uysal were selected as the Li-Fi Reference Channel Models by the IEEE 802.15.13 and the IEEE 802.11bb Task Groups. His current research interests include optical wireless communications, indoor visible light communications, underwater visible light communications, vehicular visible light communications, and channel modeling. He is a Telecommunications Advisory Board Member of the Cambridge Scholars Publishing, an Academic Editor of *IntechOpen*, and an Editorial Board Member of *Optical Communications* (Clausius Scientific Press).

SADI SAFARALIEV received the B.Sc. degree in physics from Middle East Technical University, Ankara, Turkey, in 2014, with a focus on optoelectronics. He is currently pursuing the M.Sc. degree in electrical and electronics engineering with Ozyegin University, Istanbul, Turkey, under supervision of Prof. M. Uysal. His M.Sc. thesis is on channel modeling for visible light communications (VLC).

Since 2014, he has been a Senior Optical Design Engineer with Vestel Electronics Corporation, Manisa, Turkey, where he is mainly responsible for the optical design of LED lighting products, from concept to mass production, including designing of optical components (e.g., reflectors and lenses), benchmarking, and researching new products. His research interests include optical engineering of lighting products, imaging and non-imaging components, and optoelectronics.

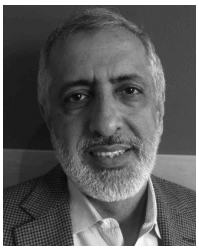

SADIQ M. SAIT was born in Bengaluru, India. He received the bachelor's degree in electronics engineering from Bangalore University, in 1981, and the master's and Ph.D. degrees in electrical engineering from the King Fahd University of Petroleum & Minerals (KFUPM), in 1983 and 1987, respectively, where he is currently a Professor of computer engineering and the Director of the Center for Communications and IT Research, Research Institute. He has authored over 200 research papers, contributed chapters to technical books, granted several U.S. patents, and lectured in over 25 countries. He is also the Principle Author of two books. He received the Best Electronic Engineer Award from the Indian Institute of Electrical Engineers, Bengaluru, in 1981.

MURAT UYSAL received the B.Sc. and the M.Sc. degrees in electronics and communication engineering from Istanbul Technical University, Istanbul, Turkey, in 1995 and 1998, respectively, and the Ph.D. degree in electrical engineering from Texas A&M University, College Station, TX, in 2001.

He is currently a Full Professor and the Chair of the Department of Electrical and Electronics Engineering, Ozyegin University, Istanbul, Turkey. He also serves as the Founding Director of the Center of Excellence in Optical Wireless Communication Technologies (OKATEM). Prior to joining Ozyegin University, he was a tenured Associate Professor with the University of Waterloo, Canada, where he still holds an Adjunct Faculty position. His research interests include the areas of communication theory and signal processing, with a particular emphasis on the physical layer aspects of wireless communication systems in radio and optical frequency bands. His distinctions include the Marsland Faculty Fellowship, in 2004, the NSERC Discovery Accelerator Supplement Award, in 2008, the University of Waterloo Engineering Research Excellence Award, in 2010, the Turkish Academy of Sciences Distinguished Young Scientist Award, in 2011, and the Ozyegin University Best Researcher Award, in 2014, among others. He has served as the Chair of the Communication Theory Symposium of the IEEE ICC 2007, the Communications and Networking Symposium of the IEEE CCECE 2008, and the Communication and Information Theory Symposium of the IWCMC 2011, the TPC Co-Chair of the IEEE WCNC 2014, and the General Chair of the IEEE IWOW 2015. Over the years, he has served on the technical program committee of more than 100 international conferences and workshops in the communications area. He was an Editor of the IEEE TRANSACTIONS ON COMMUNICATIONS, IEEE TRANSACTIONS ON VEHICULAR TECHNOLOGY, IEEE COMMUNICATIONS LETTERS, *Wireless Communications and Mobile Computing* (WCMC) journal (Wiley), and *Transactions on Emerging Telecommunications Technologies* (ETT, Wiley) and the Guest Editor of the IEEE JSAC SPECIAL ISSUES ON OPTICAL WIRELESS COMMUNICATION, in 2009 and 2015. He was involved in the organization of several IEEE conferences at various levels. He currently serves on the Editorial Board of the IEEE TRANSACTIONS ON WIRELESS COMMUNICATIONS.